Electronic Supplemental Material
Consensus and Polarizsation in Competing Complex Contagion Processes

Vítor V. Vasconcelos and Simon A. Levin
Department of Ecology and Evolutionary Biology, Princeton University, Princeton (NJ), USA

Flávio L. Pinheiro
Nova Information Management School (NOVA IMS),
Universidade Nova de Lisboa, Lisboa, Portugal and
The MIT Media Lab – Massachusetts Institute of Technology, Cambridge (MA), USA
(Dated: May 11, 2019)

GENERAL TWO COMPETING OPINIONS MODEL

We consider a finite population of Z individuals, possibility structured. Each individual holds one of two opinions, A or B. At each time-step, a random individual is selected to potentially update their strategy. Individuals revise their opinions by considering the configuration of their neighbourhood. An individual i with opinion $X = A$ or B changes to a different opinion $Y = B$ or A with probability

$$p_i^{X\to Y} = f_i^{XY}\left[\frac{n_i^Y}{z_i}\right], \tag{1}$$

where n_i^Y is the number of neighbours of i with opinion Y and z_i the size of their neighbourhood. The form of f_i^{XY} encapsulates the complexity of opinion Y when being acquired by an individual i that holds opinion X, given their environment (current neighbours opinion distribution). This transition probability can be seen as deriving from a fractional threshold model where each opinion has a different threshold distribution, $d_{XY}[M]$. In the threshold models, an opinion is adopted if, in the neighbourhood of an individual, there is at least a fraction M of individuals with that opinion (e.g., $M = 1/2$ corresponds to simple majority). In such a case, the probability an individual changes strategy is the probability that the threshold is below the current fraction of neighbours, such that $f_i^{XY}[n_i^Y/z_i] = \int_0^{n_i^Y/z_i} d_{XY}[M]dM$. This creates a dynamical and stochastic process in which the number of individuals with opinion A, k, and that of those with opinion B, $Z-k$, evolve in time. In the main text, we assume a homogeneous populations (i.e., non-subjective complexity) and we characterizse the complexity of an opinion by a single parameter, α_{XY}, which controls the functional form of f^{XY}. However, we allow for competition between opinions with different complexities ($\alpha_{AB} \neq \alpha_{BA}$). Figure 1 shows how $p_i^{X\to Y}$ changes with the density of Y individuals for different values of α_{XY}.

GENERAL MEAN-FIELD DESCRIPTION

Let us start by considering the case of a single finite and fully connected well-mixed population. The neighbourhood of each individual, is, thus, comprised of the entire population, making $p_i^{X\to Y} = f^{XY}\left[k^Y/(Z-1)\right]$, where k^Y is the number of individuals in the population with strategy Y. The dynamical process becomes fully described upon the computation of the transition probabilities between the different available configurations, $k \equiv k^A$, each corresponding to a possible composition of opinions in the population. The probability that the number of individuals with opinion A increases, T_k^+, and decreases, T_k^-, by one is given, respectively, by

$$T_k^+ = \frac{Z-k}{Z} f^{BA}\left[\frac{k}{Z-1}\right] \text{ and} \tag{2a}$$

$$T_k^- = \frac{k}{Z} f^{AB}\left[\frac{Z-k}{Z-1}\right]. \tag{2b}$$

For sufficiently large Z, $x \equiv k/Z$ can be approximated by a continuous process and the evolution of its probability density function, ρ, is well approximated by Fokker-Planck equation [4, 5],

$$\begin{aligned}\frac{\partial \rho}{\partial t} = &-\frac{\partial}{\partial x}\left[(T^+[x] - T^-[x])\rho\right] \\ &+ \frac{1}{2Z}\frac{\partial^2}{\partial^2 x^2}\left[(T^+[x] + T^-[x])\rho\right]\end{aligned} \tag{3}$$

where $T^{\pm}[x] = T^{\pm}_{xZ}$. In turn, this equation is equivalent to a Langevin description

$$\dot{x} = g[x] + \sqrt{D[x]}\Gamma(t), \tag{4}$$

where the so-called gradient of selection $g[x]$ [7] is given by

$$\begin{aligned} g[x] &= T_k^+ - T_k^- \\ &= (1-x) f^{BA}[x] - x f^{AB}[1-x] \end{aligned} \tag{5}$$

and the non-homogeneous diffusion, $D[x]$, is given by

$$\begin{aligned} D[x] &= \frac{T^+[x] + T^-[x]}{2Z} = \\ &= \frac{(1-x) f^{BA}[x] + x f^{AB}[1-x]}{2Z} \end{aligned} \tag{6}$$

In the limit of very large populations, $Z \rightarrow \infty$, the dynamics becomes described by a non-linear differential equation that can be written in the form

$$\dot{x} = (1-x) f^{BA}[x] - x f^{AB}[1-x]. \tag{7}$$

Let us derive the general properties of this equation. Notice that the equation is symmetric for interchanging A for B and x for $1-x$, which simplifies our analysis.

Fixed points

Following the same strategy as in the main text, we define $h^{BA}[x] \equiv f^{BA}[x]/x$ and $h^{AB}[1-x] \equiv f^{AB}[1-x]/(1-x)$. In that case, we can conveniently rewrite Equation (7) as

$$\dot{x} = x(1-x)\left(h^{BA}[x] - h^{AB}[1-x]\right). \tag{8}$$

Notice that our definition of $h^{BA}[x]$ causes the need of particular care for what is happening around $x=0$. Indeed, $h^{BA}[x]$ can have poles at that point – the obvious case is for non-zero $f^{BA}[0]$. However, it does not lose its meaning in the light of Equation (7): indeed the term $h^{BA}[x] - h^{AB}[1-x]$ can be seen as a force generated by a potential that describes the evolution of contact processes, and the non-zero $f^{BA}(0)$ is just creating an infinite barrier to fixation at $x=0$, which renders $x=0$ unstable (see non-conservative evolutionary dynamics section in [2]). However, if $f^{BA}(x)$ grows super-linearly from zero, i.e., $f^{BA}(x) \sim O(x^{\epsilon})$ with $\epsilon \geq 1$ and $f^{BA}(0)=0$, then $h^{BA}(x)$ can be analytically extended to a finite value. Thus, we can have two natural fixed points $x^*=0$ and $x^*=1$. Their existence is given by $f^{BA}[0]=0$ and $f^{AB}[1]=0$, respectively. Then, additional fixed points can occur depending on the behaviour of the term

$$h[x] \equiv h^{BA}[x] - h^{AB}[1-x]. \tag{9}$$

Furthermore, notice that the stability of the fixed points will depend on derivatives of $f^{BA}(x)$ which, in the fraction threshold interpretation, corresponds to the threshold distribution itself, as $\frac{d}{dx} f^{XY}(x) = \frac{d}{dx}\int_0^x d_{XY}(M)dM = d_{XY}(x)$, via the fundamental theorem of calculus.

Stability of $x^*=0$

Whenever $\dot{x}[0] > 0$, which requires $f^{BA}[0] > 0$, $x=0$ is not a fixed point and the system will move away from it. If $f^{BA}[0]=0$ then the stability of $x^*=0$ can be determined by studying the sign of $d\dot{x}/dx$.

$$\begin{aligned}\frac{d\dot{x}}{dx}[x] = &- f^{BA}[x] + (1-x)\frac{df^{BA}}{dx}[x] \\ &- f^{AB}[1-x] + x\frac{df^{AB}}{dx}[1-x].\end{aligned} \tag{10}$$

At the fixed point it reads

$$\frac{d\dot{x}}{dx}[0] = \frac{df^{BA}}{dx}[0] - f^{AB}[1]. \tag{11}$$

Whenever ${}^{df^{BA}}\!/_{dx}[0] > f^{AB}[1]$, $x^*=0$ is unstable. For ${}^{df^{BA}}\!/_{dx}[0] < f^{AB}[1]$, $x^*=0$ is stable. For ${}^{df^{BA}}\!/_{dx}[0] = f^{AB}[1]$, higher derivatives must be accounted for. This shows that the stability of the boundaries is mostly determined by the rate of change of f^{BA} when there are only a few individuals of type A compared with the contagion probability of Bs by As when Bs dominate.

Stability of $x^*=1$

Because of the symmetry mentioned, the stability of $x^*=1$ is determined by the sign of

$$\frac{d\dot{x}}{dx}[1] = \frac{df^{AB}}{dx}[1] - f^{BA}[0]. \tag{12}$$

Whenever, ${}^{df^{AB}}\!/_{dx}[1] > f^{BA}[0]$, $x^*=1$ is unstable. For ${}^{df^{AB}}\!/_{dx}[1] < f^{BA}[0]$, $x^*=0$ is stable. For ${}^{df^{AB}}\!/_{dx}[1] = f^{BA}[0]$, higher order derivatives must be accounted for.

Internal fixed points

Because $\dot{x}$ is continuous in x, whenever both fixed points are stable, i.e., ${}^{df^{BA}}\!/_{dx}[0] < f^{AB}[1]$ and ${}^{df^{AB}}\!/_{dx}[1] < f^{BA}[0]$, there is at least one unstable fixed point in $(0,1)$. If both are unstable, there is at least one stable fixed point in $(0,1)$. More, whenever $h^{BA}[x]$ crosses $h^{AB}[1-x]$ from above, there is a stable fixed point. When $h^{BA}[x]$ crosses $h^{AB}[1-x]$ from below, there is an unstable fixed point.

MEAN-FIELD DESCRIPTION – MS MODEL

In the main text we discuss a model where

$$f_i^{XY}\left[\frac{n_i^Y}{z_i}\right] = \left(\frac{n_i^Y}{z_i}\right)^{\alpha_{XY}}, \tag{13}$$

which contains the key properties of the complex contagion properties of monotonic functions.

We start by considering the case of a single finite and fully connected well-mixed population. The neighbourhood of each individual is, thus, comprised of the entire population. Following the procedure described in section above, we can write Eq.(7) as

$$\dot{x} = x(1-x)(x^{\alpha_{BA}-1} - (1-x)^{\alpha_{AB}-1}), \qquad (14)$$

The system described by Eq.(14) above has, for $\alpha_{XY} \neq 1$, the two trivial solutions at $x = 0$ and $x = 1$ and an additional internal fixed point that can be inspected by solving

$$x^{\alpha_{BA}-1} - (1-x)^{\alpha_{AB}-1} = 0 \qquad (15)$$

In such a case, and taking $\gamma = (\alpha_{BA} - 1)/(\alpha_{AB} - 1)$, the solutions can be found by solving the transcendental equation

$$1 - x = x^{\gamma} \qquad (16)$$

whose LHS and RHS are graphically depicted in Figure 2. The stability nature of the internal fixed point is unstable when both $\alpha_{XY} > 1$ (lower left quadrant) and stable when both $\alpha_{XY} < 1$ (top right quadrant). In the regions bounded by $\alpha_{AB} > 1 \wedge \alpha_{BA} < 1$ and $\alpha_{AB} < 1 \wedge \alpha_{BA} > 1$, there are no internal fixed points (gray areas). We prove this below. Two other trivial dynamics exist in the $\alpha_{AB} \times \alpha_{BA}$ parameter-space: i) when $\alpha_{AB} = \alpha_{BA} = 1$, $g(x) = 0$, so every state corresponds to a fixed point and a finite population would evolve under neutral drift, since $D(x) = (x(1-x))/Z \neq 0$, and ii) when $\alpha_{AB} = \alpha_{BA} = 0$ in which case $g(x) = (1-2x)$ and $D(x) = 1/2Z$, which reduces the problem to an Ornstein-Uhlenbeck process.

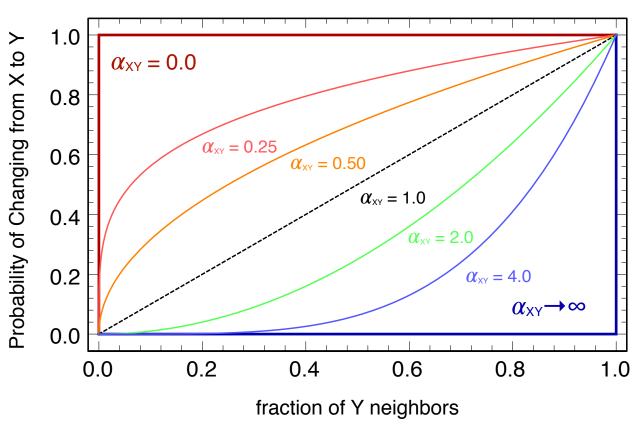

Figure 1. Probability that individuals update their opinion from X to Y as a function of the abundance of opinion Y individuals in the neighbourhood of an X. Different colours show scenarios with different values of α_{XY}.

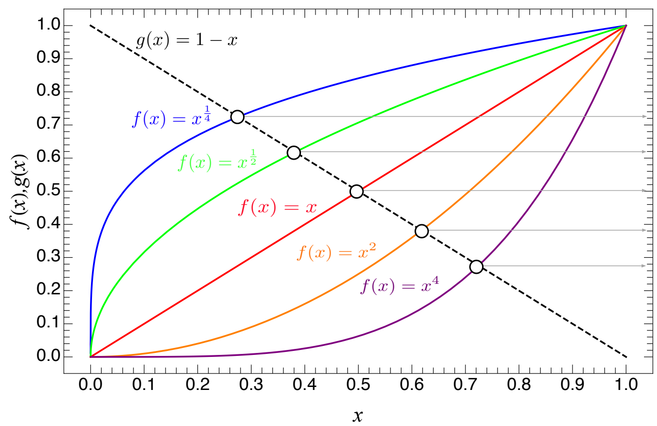

Figure 2. Graphical Depiction of Equation 16 solutions, where $f(x) = x^{\gamma}$ and $g(x) = 1 - x$.

Stability of edges ($x^* = 0$ and $x^* = 1$)

For $x^* = 0$, we use Eq.(11) and we note that $f^{AB}[1] = 1$ and the first derivative is given by $\frac{df^{BA}}{dx}[x] = \alpha_{BA} x^{\alpha_{BA}-1}$. Furthermore,

$$\frac{df^{BA}}{dx}[x] = \alpha_{BA} x^{\alpha_{BA}-1} \xrightarrow{x\to 0} \begin{cases} 0 & \alpha_{BA} > 1 \\ 1 & \alpha_{BA} = 1 \\ \infty & \alpha_{BA} < 1 \end{cases}. \qquad (17)$$

This solves stability for $\alpha_{BA} > 1$ and $\alpha_{AB} < 1$. For $\alpha_{BA} = 1$, we use the second derivative

$$\begin{aligned} \frac{d^2\dot{x}}{dx^2}[x] = & -2\frac{df}{dx}^{BA}[x] + 2\frac{df}{dx}^{AB}[1-x] \\ & + (1-x)\frac{d^2 f^{BA}}{dx^2}[x] - x\frac{d^2 f^{AB}}{dx^2}[1-x], \end{aligned} \qquad (18)$$

which for $x = 0$ and $\alpha_{BA} = 1$, gives

$$\frac{d^2\dot{x}}{dx^2}[0] = -2 + 2\alpha_{AB}. \qquad (19)$$

This is positive for $\alpha_{AB} > 1$ and negative for $\alpha_{AB} < 1$. For both $\alpha_{BA} = \alpha_{AB} = 1$, $\dot{x} = 0$ for all $x \in [0, 1]$. Thus,

- $x^* = 0$ is stable iff either $\alpha_{BA} > 1$ or both $\alpha_{BA} = 1$ and $\alpha_{AB} < 1$,
- $x^* = 0$ is unstable iff either $\alpha_{BA} < 1$ or both $\alpha_{BA} = 1$ and $\alpha_{AB} > 1$,
- $x^* \in [0, 1]$ is neutrally stable iff $\alpha_{BA} = \alpha_{AB} = 1$.

Equivalently, for $x^* = 1$, we get

- $x^* = 1$ is stable iff either $\alpha_{AB} > 1$ or both $\alpha_{AB} = 1$ and $\alpha_{BA} < 1$,
- $x^* = 1$ is unstable iff either $\alpha_{AB} < 1$ or both $\alpha_{AB} = 1$ and $\alpha_{BA} > 1$,
- $x^* \in [0, 1]$ is neutrally stable iff $\alpha_{BA} = \alpha_{AB} = 1$.

Internal fixed point

The equation for the internal fixed point, $y \in (0,1)$, is given by the roots of $h[x]$ in Eq.(9). In this case,

$$y \in (0,1): \; y^{\alpha_{BA}-1} = (1-y)^{\alpha_{AB}-1}. \tag{20}$$

If any of the α_{XY} is 1, solution is $y = 1$, which is the boundary, which we already analyzed. Otherwise, we can reduce the equation above to

$$y \in (0,1): \quad 1 - y = y^{\gamma}, \tag{21}$$

where $\gamma \equiv {}^{(\alpha_{BA}-1)}/_{(\alpha_{AB}-1)}$. Notice that for $\alpha_{XY} > 0$, $\gamma \in \mathbb{R}$. More, the parameterizsation $\alpha_{BA} = r\cos\theta + 1$ and $\alpha_{AB} = r\sin\theta + 1$ yields $\gamma = \text{cotan}\theta$, which means that any point with the same θ will have the same root, as we can see in Figure 1 of the main text. Eq.(21) corresponds to the intersection of a straight line $(1-y)$ with a power y^{γ}. Thus, y exists in $(0,1)$ and is unique iff $\gamma > 0$. Thus, through the definition of γ, we get

$$\begin{aligned} \gamma > 0 \Leftrightarrow \frac{\alpha_{BA}-1}{\alpha_{AB}-1} > 0 \Leftrightarrow \\ \Leftrightarrow (\alpha_{BA} > 1 \text{ and } \alpha_{AB} > 1) \\ \text{or } (\alpha_{BA} < 1 \text{ and } \alpha_{AB} < 1). \end{aligned} \tag{22}$$

To get the stability of y, we either use the results presented in the general section and the unicity of the root, or we look at the linearizsation of $\dot{x}$ near it.

$$\begin{aligned} \frac{d\dot{x}}{dx}[y] = &-(1-y)^{\alpha_{AB}-1}(1-y-\alpha_{AB}y) \\ &- y^{\alpha_{BA}-1}(y-(1-y)\alpha_{BA}). \end{aligned} \tag{23}$$

Using the property of the fixed point as $(1-y)^{\alpha_{AB}-1} = y^{\alpha_{BA}-1}$ or $1-y = y^{\gamma}$ we get

$$\begin{aligned} \frac{d\dot{x}}{dx}[y] = &y^{\alpha_{BA}-1}((1-y)(\alpha_{BA}-1) \\ &+ y(\alpha_{AB}-1)). \end{aligned} \tag{24}$$

In the intervals where the root exists, we get

- $(\alpha_{BA} > 1 \text{ and } \alpha_{AB} > 1) \Rightarrow \frac{d\dot{x}}{dx}[y] > 0$, the point is unstable,
- $(\alpha_{BA} < 1 \text{ and } \alpha_{AB} < 1) \Rightarrow \frac{d\dot{x}}{dx}[y] < 0$, the point is stable.

Expected Time to Reach Consensus

Another quantity of interest is the time required to reach a consensus (τ_k) when starting from configuration k. For $\alpha_{XY} > 0$, the system has two absorbing states, $k = 0$ and $k = Z$, so it represents an Absorbing Markov Chain. Thus, the time to consensus (fixation) starting from configuration k can be formally computed as [8]

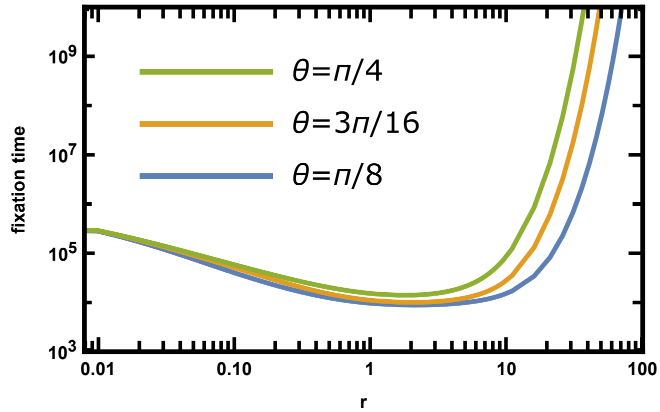

Figure 3. Fixation time in the consensus regime. For low values of r the dynamicsisare neutral and the expected time given by Eq. (26). As r increases, the coordination-like dynamics makes the system evolve towards one of the consensuses. However, for very large r the dynamics freeze.

$$\tau_k = -\tau_1 \sum_{j=k}^{Z-1} \prod_{m=1}^{j} \gamma_m + \sum_{j=k}^{Z-1} \sum_{l=1}^{j} \frac{1}{T_l^+} \prod_{m=l+1}^{j} \gamma_m \tag{25a}$$

$$\tau_1 = \frac{1}{1 + \sum_{j=1}^{Z-1} \prod_{m=1}^{j} \gamma_m} \sum_{j=1}^{Z-1} \sum_{l=1}^{j} \frac{1}{T_l^+} \prod_{m=l+1}^{j} \gamma_m \tag{25b}$$

where $\gamma_m = T_m^-/T_m^+$. Alternatively, for a higher dimensional process, it can be computed as $t_k = \sum_{l=1}^{Z-1} N_{kl}$, where $[N_{ij}]$ is the fundamental matrix of the chain, given by $[N_{ij}] = [((1-Q)^{-1})_{ij}]$, and Q is the transition matrix between the transient states, $k = 1, \ldots, Z-1$ [9]. For $\alpha_{XY} = 1$, the process evolves under neutral drift, $T_m^+ = T_m^-$, making $\gamma_m = 1$ and the average fixation time is given by

$$\tau_k^0 = (Z-1)(Z(H_{Z-1} - H_{Z-k}) + k(H_{Z-k} - H_k) + 1) \tag{26}$$

where $H_n = \sum_{l=1}^{n} 1/l$ is the harmonic number that increases logarithmically with n as $H_n = \eta + \ln(n) + 1/(2n) + O(n^{-2})$, where $\eta \approx 0.5772156649$ is the Euler-Mascheroni constant. For $k = 1$ it reduces to $t_1^0 = (Z-1)H_{Z-1}$.

An interesting result in our model relates to the fact that, for very high complexities, the process slows down. That has to do high the need of very high consensus for a state change. Thus, for a fixed $\theta \in (0, \pi/4)$, negative values of r correspond to the polarizsation region, where fixation times are very high. As r goes to zero the fixation times approach neutral and, as it becomes positive, in the consensus region, there is a value of r that minimizses the fixation time (see Fig.3), corresponding to the fastest dynamics characterizsed by the same coordination

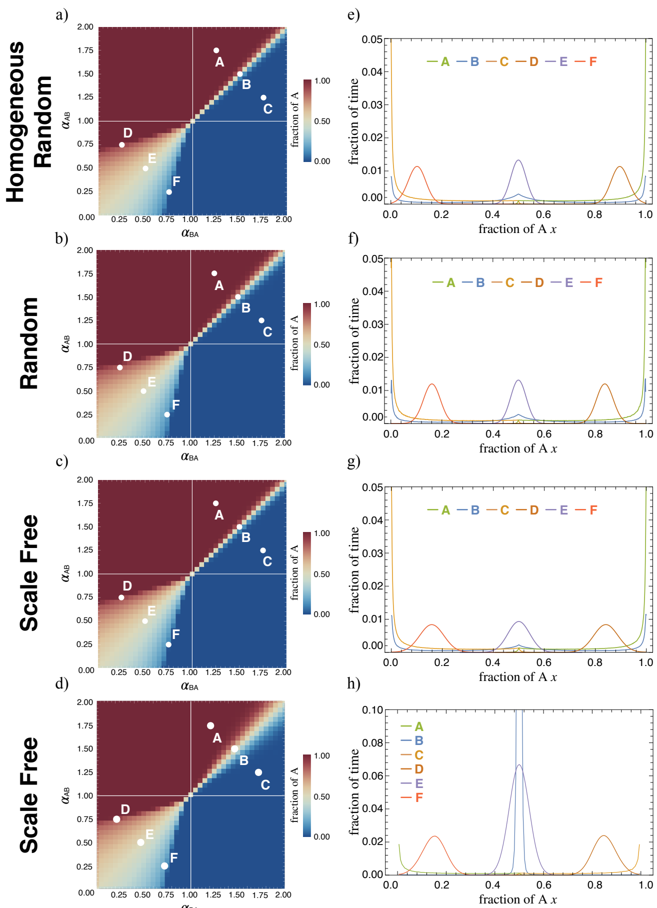

Figure 4. Average final fraction of opinion A and quasi-stationary distributions in structured populations. Panels a) and e) show the results in *Homogeneous Random Networks*, b) and f) in *Random Networks*, c) and g) in *Scale-free Networks*, d) and h) in *Modular* networks. All structures have $Z = 10^3$ nodes and an average degree of 4. Panels a–d show the average final fraction of opinion A when evolution starts from a configuration with equal abundance of opinions A and B. Blue/Red indicates regions dominated by opinion B/A. Panels e–h show the quasi-stationary distribution along six different combinations of the parameters α_{AB} and α_{BA}, indicated in panels a–d. Results are the average over 10^4 independent simulations for each pair of parameters, and the results correspond to the average observed value after 2.5 million Monte Carlo Steps. The quasi-stationary distribution show the fraction of time the population spent in which configuration.

barrier (same unstable fixed point of the deterministic dynamics).

STRUCTURED POPULATIONS

In this work we have explored the effect of three different population structures. We have used complex networks as a way to model population structure. In that sense, vertices/nodes correspond to individuals and edges/links indicate the existence of a social tie between a pair of individuals. Following past works, we have used three network topologies, namely, *Homogeneous Random Networks* (**HRND**), *Random Networks* (**ER**), *Scale-free Networks* (**SF**), and Modular networks. These networks span a wide range of network heterogeneity (degree variance).

ER networks were generated through the Erdős–Rényi algorithm [3]. Starting from a set of Z unconnected nodes, pairs of nodes are sequentially connected with probability p. We stop when all pairs of nodes have been tested. Moreover, we discard networks in which there are disconnected components. We choose a value of p that guarantees the network will have the desired average degree. **HRND** are generated by randomly swapping the ends of edges from an initially regular graph [6] until all topological correlations vanish. **SF** are created using the *Barabási-Albert* algorithm of growth and preferential attachment [1]. Starting with m fully connected nodes, the remaining $Z - m$ nodes are sequentially added to the network and attached to $m - 1$ pre-existing nodes but preferentially to those with a higher degree. We use $m = 3$, leading to a network with an average degree of 4. Finally, Modular networks are generated by connecting at random a number q of nodes from two independently generated scale-free networks with $Z/2$ nodes. In the manuscript, we choose $q = 20$ to study a scenario of a weakly connected two-component modular network.

Figure 4a–d shows the average final fraction of opinion A in the domain defined by $0 \leq \alpha_{AB} \leq 2$ and $0 \leq \alpha_{BA} \leq 2$. Overall we observe that results are qualitatively similar among the three structures, and with the results obtained in well-mixed populations. However, two noteworthy differences need to be mentioned. First, in region (i), that concerns the consensus/coordination dynamical regime, the transition is sharper for homogeneous networks, and becomes wider as networks become more heterogeneous. Second, there is a considerable range of parameters in region (**iv**), which concerns the polarizsation/co-existence dynamical regime, where population structure leads to a dominance-like dynamics, which contrasts with the findings in well-mixed populations.

Figure 4e–h shows the quasi-stationary distributions for six combinations of the complexity parameters, as indicated in panels a–d of Figure 4a–d. These results show another difference prompted by the different network structures, and that concerns the observed diffusion levels:, as the peaks in the polarizsation levels have different variances.

Following the results in Figure 1 of the main text, Figure 5a–d shows the average fixation times for different combinations of the parameters α_{BA} and α_{AB}. To complement these results we also show the average final fraction of opinion A for the same combination of parameters in Figure 5e–h.

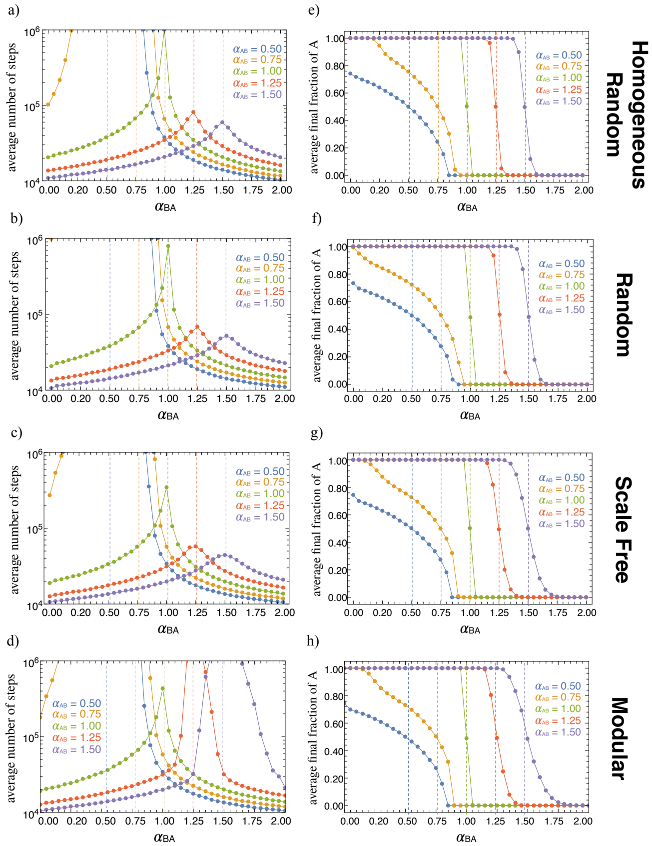

Figure 5. Long-run properties of the distribution. Panels a, b, c, and d show the average number of steps to fixation in one of the monomorphic states, with an upper bound of 2.5 Million Monte Carlo Steps. Panels e, f, g, and h show the expected final fraction of individuals of type A.

[1] Albert, R., and A.-L. Barabási (2002), Rev. Mod. Phys. **74** (1), 47.

[2] Chalub, F. A., and M. O. Souza (2018), J Theor Biol.

[3] Erdos, P., and A. Rényi (1960), Publications of the Mathematical Institute of the Hungarian Academy of Sciences **5** (1), 17.

[4] Gardiner, C. (2009), *Stochastic methods*, Vol. 4 (springer Berlin).

[5] Risken, H. (1996), in *The Fokker-Planck Equation* (Springer) pp. 63–95.

[6] Santos, F. C., J. F. Rodrigues, and J. M. Pacheco (2005), Phys. Rev. E **72** (5), 056128.

[7] Sigmund, K., and M. A. Nowak (1999), Curr. Bio.l **9** (14), R503.

[8] Traulsen, A., and C. Hauert (2009), Reviews of Nonlinear Dynamics and Complexity **2**, 25.

[9] Van Kampen, N. G. (1992), *Stochastic processes in physics and chemistry*, Vol. 1 (Elsevier).